OURNAL OF MATERIALS SCIENCE 4 (1969) 565–569

Ferroelectric Domains and Growth Striae in Barium Sodium Niobate Single Crystals

B. COCKAYNE, M. CHESSWAS, J. G. PLANT, A. W. VERE
Royal Radar Research Establishment, Malvern, Worcs, UK

Received 20 November 1968

The relationship between the ferroelectric domain structure and growth striae is examined in barium sodium niobate ($Ba_2NaNb_5O_{15}$) single crystals. Growth striae stabilise a particular form of domain structure and are further shown to be caused by temperature fluctuations occurring in the melts from which such crystals are grown. These fluctuations and the associated striae can be eliminated by reducing the melt level in the crucible used to contain the molten material. Evidence is presented to show that this effect cannot simply be regarded as a reduction in the Rayleigh Number of the melt system, as convective effects occurring in the gas ambient above the melt also exert an influence.

1. Introduction

$Ba_2NaNb_5O_{15}$ is one of a group of ferroelectric niobates, generally referred to as the tetragonal tungsten bronze structures because of their similarity in crystal structure to $K_{0.6}WO_3$. They exhibit useful electro-optic and second harmonic generation properties [1], and $Ba_2NaNb_5O_{15}$ is of particular interest in frequency doubling applications because its conversion efficiency and resistance to optical damage [2] are superior to those of other known materials, e.g. $LiNbO_3$.

The growth of $Ba_2NaNb_5O_{15}$ single crystals by the vertical pulling technique has already been described by Van Uitert *et al* [3] who reported the occurrence of a multidomain ferroelectric structure. The present work examines factors which affect the formation and control of both this defect and another optical inhomogeneity, namely growth striae, which cause localised changes in the refractive index of the material.

2. Experimental Details

The vertical pulling apparatus used for crystal growth was identical to that already described for the growth of sapphire single crystals [4], with the exception that the crucible and heat shields were constructed from platinum rather than iridium. Melts of the required molecular composition were prepared from carefully dried $Ba(NO_3)_2$, $NaNO_3$ and Nb_2O_5 supplied as Optran grade material by British Drug Houses Ltd. The crucible employed was 3.75 cm in diameter × 3.15 cm in height with a wall thickness of 0.15 cm. The gas ambient was 100% O_2 and the crystal pull and rotation rates were within the respective ranges 2 to 12 mm/h and 0 to 120 rpm. All observations were made on [001] growth axis crystals, since crystals grown on other axes are more susceptible to cracking.

In order to facilitate the movement of thermocouple probes during temperature measurements in the system, the apparatus was slightly modified. A narrow tangential slot was cut next to the circular hole normally present for insertion of the seed crystal into the heat shield surrounding the growing crystal, and the thermocouples were inserted through this slot. Pt – Pt/13% Rh thermocouples, made from 0.375 mm wire, were used for determining the temperature both within and above the melt. A maximum of two thermocouples was employed at any one time and these were rigidly supported in silica tubes and mounted upon micromanipulators capable of independent translation in three orthogonal directions. In this way the temperature at any given point in the melt or gas ambient could be measured. The output from the thermocouples was continuously monitored on variable chart speed recorders in the manner previously described [5] using an R/C filter circuit to eliminate rf interference.

The ferroelectric domain structure on (001) surfaces was revealed by etching the crystal sections in phosphoric acid at a temperature of 300° C for a period of 3 h. Photomicrographs of these structures were obtained using reflected light. A domain etchant is not available for (100) surfaces but the domains are visible at temperatures just below the Curie point (560° C) when such sections are viewed in transmission under plane polarised light.

3. Results and Discussion

3.1. The Ferroelectric Domain Structure and Growth Striae

One particular ferroelectric domain distribution in Czochralski grown $Ba_2NaNb_5O_{15}$ has been identified by Van Uitert *et al* [3]. This has been observed principally in [001] axis crystals where the domains are distributed in a "stacked saucer" arrangement in which adjacent "saucers" are of opposite domain. When this configuration is intersected by the (001) plane of the crystal, a concentric ring pattern is produced (fig. 1). The present work confirms that when such crystals are sectioned parallel to the growth axis, the domain boundaries are revealed as striae approximately 10^{-3} cm apart. These striae, depicted in fig. 2, are parallel to the solid/liquid interface of the growing crystal and are generally either very slightly concave or convex with respect to the melt. The gross striae in fig. 2 coincide with the position of the growth interface at times when manual alteration of the power input to the crucible was necessary in order to control the crystal diameter.

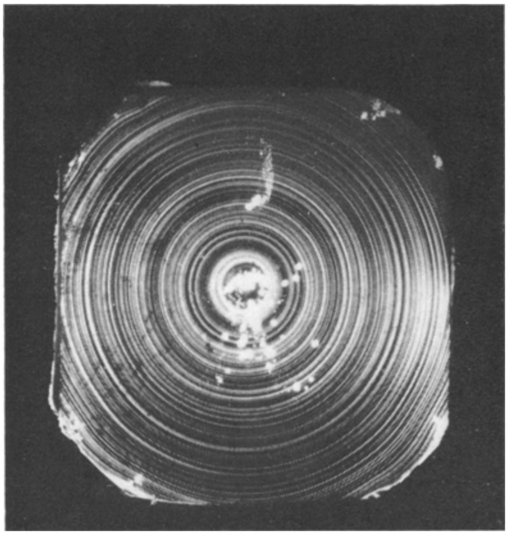

Figure 1 Concentric ring domain structure observed on (001) sections of [001] axis $Ba_2NaNb_5O_{15}$ single crystals grown from impure melts (× 6).

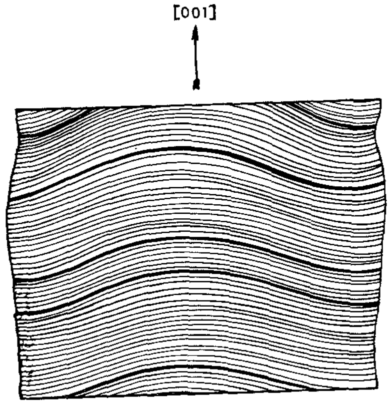

Figure 2 A schematic representation of striae observed in (100) crystal sections cut parallel to the [001] growth axis.

In addition, the present work has established that crystals grown from either purer or more stoichiometric melts, achieved by using starting material in the form of previously grown crystals rather than the component powders, show a reduced number of domain rings on etched crystal sections cut perpendicular to the [001] growth axis (fig. 3). Improved control of growth is also achieved with the purer melts. As a

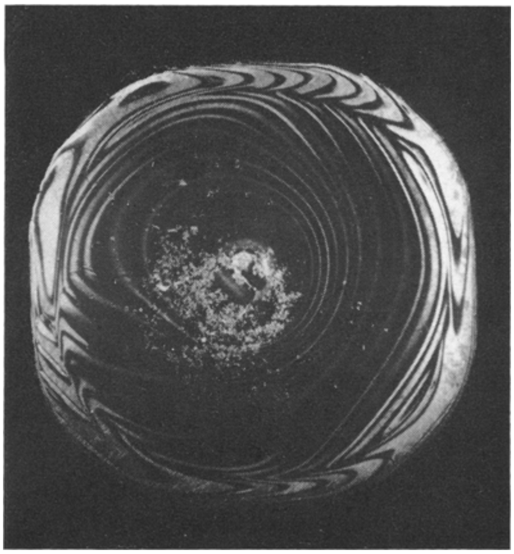

Figure 3 Concentric ring domain structure observed on (001) sections of [001] axis crystals grown from pure melts (× 6).

consequence, fewer manual power changes are required and the gross striae occur less frequently although they still coincide with the domain boundaries. The fine striae, however, become much less distinct and appear to lose all correlation with the ferroelectric domains, since their spacing remains unaltered despite the coarsening of the domain structure.

Visual observations made through crossed polaroids whilst cycling crystal sections through the Curie point (560° C) under the influence of a temperature gradient applied normal to the striae, confirm this loss of correlation between the fine straie and the domain boundaries in the purer crystals. During the heating cycle, a transformation nucleates at the hot end of the specimen (at approximately 560° C) and moves through the crystal. The transformation proceeds with a marked discontinuous stepwise motion and the step width corresponds to the spacing between the gross striae. In crystals grown from the powdered components, the discontinuous motion is much less pronounced, as the step width then corresponds to the fine striae spacing. The reverse effect is observed on cooling.

It has been reported previously that single domain $Ba_2NaNb_5O_{15}$ can be produced from multidomain crystals by the application of a DC field along the [001] axis [3], and the present work has established that (001) crystal sections poled in this manner show no evidence of the ring structure characteristic of multidomain material. Examination of (100) sections of poled crystals shows, however, that both the gross and the fine striae are unaffected by the poling process, regardless of starting material purity.

From these observations it is concluded that the striae are independent of the ferroelectric nature of the material. However, when present, they can stabilise a particular form of domain structure, i.e. the concentric ring pattern. It is well known that striae in Czochralski grown crystals represent a local compositional change and, in the present case, the ability of the striae to anchor domains is markedly dependent upon the magnitude of the compositional change within the striations. In this respect, the gross straie which represent the largest change in composition are the most effective. Striae-free crystals (see section 3.2.) adopt a random domain pattern of the type shown in fig. 4.

A mass spectrographic analysis has shown that the total impurity concentration within the crystals is less than 10 ppm, so it would appear that the compositional change at the striae is more likely to arise from deviations in stoichiometry rather than from impurities. Variations in melt stoichiometry undoubtedly occur during growth as a sodium-rich deposit accumulates on the silica envelope which encloses the crucible and afterheater system.

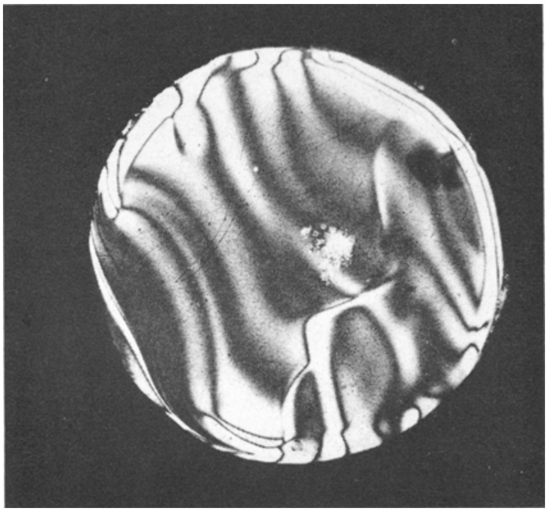

Figure 4 Random domain structure observed on (001) sections of [001] axis crystals in the absence of striae (× 6).

3.2. Growth Striae and Temperature Fluctuations

In addition to stabilising a particular arrangement of ferroelectric domains, striae cause localised changes in refractive index which greatly impair the optical properties of $Ba_2NaNb_5O_{15}$. The presence of striae in oxide single crystals grown by the Czochralski technique is not unique to $Ba_2NaNb_5O_{15}$. Similar striae have been observed in $Y_3Al_5O_{12}$, $MgAl_2O_4$, Al_2O_3 and $CaWO_4$ [5-7]. In $CaWO_4$ [5], the occurrence of striae has been correlated with temperature oscillations in the melt, which modulate the incorporation of either an impurity or an excess of one of the component oxides by producing changes in growth rate, hence the term growth striae. Fig. 5 shows that similar temperature variations, occurring as fluctuations rather than oscillations, can be detected underneath the interface of a $Ba_2NaNb_5O_{15}$ crystal growing from its own melt. The major fluctuations occur within the limits eight to twelve per

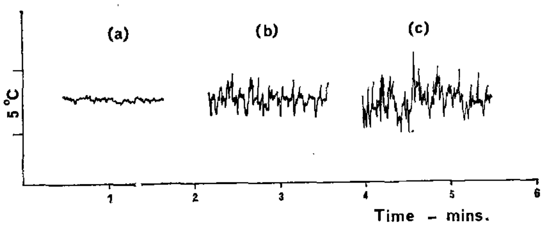

Figure 5 Temperature fluctuations detected 1 mm beneath the interface of a $Ba_2NaNb_5O_{15}$ single crystal growing from its own melt with a melt depth of (a) 1 cm (b) 2 cm (c) 3 cm.

min. This is in good agreement with the measured spacing of fine striae of 10^{-3} cm, which is equivalent to the formation of ten striae per min in a crystal grown at 0.6 cm/h. Fig. 5 also shows that the magnitude of the temperature fluctuations is dependent upon the depth of melt in the crucible. Further evidence of the correlation between striae and fluctuations in temperature is provided by the observation that crystals grown under the temperature conditions apertaining to fig. 5a are virtually free from striae, and those straie which do persist are extremely faint. Crystals grown under the temperature conditions of figs. 5b and c, however, always contain pronounced striae.

3.3. Temperature Fluctuations and Temperature Gradients

In an earlier paper [5], it was shown that temperature variations in molten oxides are due to unstable thermal convection which occurs when the Rayleigh number of the melt, R, exceed a certain critical value. R is a dimensionless parameter, defined elsewhere [5, 10] which is directly proportional to the vertical temperature gradient in the liquid and the fourth power of the liquid depth. For gas fluid media, published data suggest that R_{critical} is approximately 2×10^4 [8] but for liquids the value is likely to be an order of magnitude lower [9]. R is estimated to have an approximate value of 10^6 for a 3 cm depth of molten $CaWO_4$ contained in a crucible of identical dimensions to that used here and subjected to a vertical temperature gradient of 100° C/cm. Under these conditions temperature oscillations are produced and a regular spoke-like convection pattern is observed on the melt surface. During the present studies, similar oscillations and convection patterns have been produced in molten $Ba_2NaNb_5O_{15}$ with a melt depth of 3 cm and a vertical temperature gradient in the melt of 70° C/cm. However, considerably lower gradients are required to prevent the crystals cracking during growth, and the actual temperature gradients measured in the apparatus during crystal growth of $Ba_2NaNb_5O_{15}$ are listed in table I. These results show that a reduction in the depth of melt, which reduces the temperature fluctuations causing striae (fig. 5), also lowers the temperature gradient in the melt, although the effect is minimal when the depth is decreased below 2 cm. This evidence suggests that the small amplitude of the temperature fluctuations in fig. 5a is due to R having been reduced below the critical value for the onset of convective instability by the combined effect of lower temperature gradient and reduced melt depth. In this case, the latter effect would predominate, as a change in melt depth from 3 cm to 1 cm decreases R by nearly two orders of magnitude. This hypothesis is not, however, entirely consistent with all the experimental observations. For instance, there is no evidence of convection patterns on the melt surface in any of the three situations illustrated by fig. 5. Furthermore, the variations in temperature occur as fluctuations typical of high R value systems rather than oscillations, despite the fact that the temperature gradient is lower in all cases than that at which oscillations were detected in a $Ba_2NaNb_5O_{15}$ melt.

TABLE I

Melt depth cm	Temp. grad. in the melt 0 to 5 mm below the crystal interface °C/cm
1	18
2	24
3	40

However, the present work has also established that temperature fluctuations are present in the gas ambient above the melt surface. These have a greater amplitude but occur with approximately the same frequency as those detected in the melt. Their amplitude is reduced as the melt level in the crucible is decreased (figs. 6 and 7). This observation is consistent with the data given in table II which shows a corresponding reduction of temperature gradient with melt level in the gas ambient. Figs. 6 and 7 also show that the fluctuations decrease in magnitude as the melt surface is approached. If the fluctuations in the gas are responsible for the changes in melt temperature, the fluctuations should be further attenuated with depth below the melt surface,

TABLE II

Melt depth cm	Temp. grad. in the gas ambient 0 to 5 mm above the melt surface °C/cm
1	50
2	120
3	130

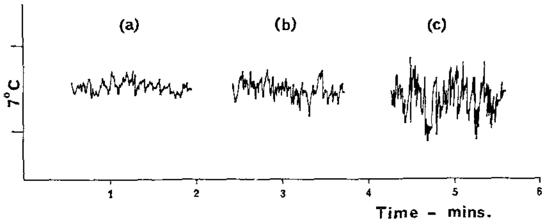

Figure 6 Temperature fluctuations detected above a $Ba_2NaNb_5O_{15}$ melt, 1 cm deep, at distances of (a) 2 mm (b) 4 mm and (c) 8 mm from the melt surface.

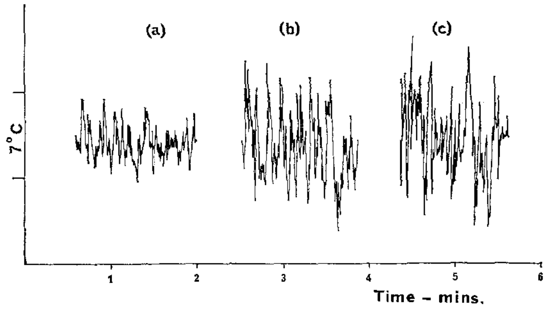

Figure 7 Temperature fluctuations detected above a $Ba_2NaNb_5O_{15}$ melt, 2 cm deep, at distances of (a) 2 mm (b) 4 mm and (c) 8 mm from the melt surface.

and this is precisely the observed case. Evidence therefore exists to suggest that under conditions of low melt temperature gradient, temperature fluctuations in the gas ambient above a $Ba_2NaNb_5O_{15}$ melt can induce temperature changes in that melt. It is significant that the value of R for a gas ambient of O_2 in the environment described here, is approximately 10^6, well within the range in which turbulent convection is observed in gases [8]; hence the detection of fluctuations rather than oscillations in the gas temperature.

It appears, therefore, that for a given size of crucible, melt depth is a parameter which can be varied in order to control temperature fluctuations and growth striae in $Ba_2NaNb_5O_{15}$. However, the reasons for its importance are complex. As the melt level is reduced, the primary effect is to increase the degree of afterheating above the melt surface. As a consequence the magnitude of temperature fluctuations in both the gas ambient and the melt are reduced thereby leading to the elimination of growth striae. As yet the relationship between temperature fluctuations in both the gas and the melt is not clearly understood but this aspect of the work is being investigated further with reference to oxide crystal growth in general.

Acknowledgements

The authors wish to thank Mr R. J. Heritage for carrying out the mass spectrographic analyses. This paper is published by permission of the Controller, HMSO.

References

1. J. J. RUBIN, L. G. VAN UITERT, and H. J. LEVINSTEIN, *J. Cryst. Growth* **1** (1967) 315.
2. J. E. GEUSIC, H. J. LEVINSTEIN, J. J. RUBIN, S. SINGH, and L. G. VAN UITERT, *Appl. Phys. Lett.* **11** (1967) 269.
3. L. G. VAN UITERT, H. J. LEVINSTEIN, J. J. RUBIN, C. D. CAPIO, E. F. DEARBORN, and W. A. BONNER, *Mat. Res. Bull.* 3 (1968) 47.
4. B. COCKAYNE, M. CHESSWAS, and D. B. GASSON, *J. Materials Sci.* **2** (1967) 7.
5. B. COCKAYNE and M. P. GATES, *ibid* **2** (1967) 118.
6. B. COCKAYNE, M. CHESSWAS, P. J. BORN, and J. D. FILBY, *ibid* 4 (1969) 236.
7. J. BASTERFIELD, M. J. PRESCOTT, and B. COCKAYNE, *ibid* 3 (1968) 33.
8. W. T. MITCHELL and J. A. QUINN, *J. A. I. Ch. E.* **12** (1966) 1116.
9. D. T. J. HURLE, E. JAKEMAN, and E. R. PIKE, *Proc. Roy Soc.* **296A** (1967) 469.
10. S. CHANDRASEKHAR, "Hydrodynamic and Hydromagnetic Stability" (Clarendon Press, Oxford, 1961).